Eur Radiol (2009) 19: 209–219
DOI 10.1007/s00330-008-1106-7

PEDIATRIC

Priyanka Jha
Soni C. Chawla
Sidhartha Tavri
Chirag Patel
Charles Gooding
Heike Daldrup-Link

Pediatric liver tumors – a pictorial review

Received: 19 December 2007
Revised: 30 May 2008
Accepted: 5 June 2008
Published online: 6 August 2008

P. Jha · S. Tavri · C. Patel · C. Gooding · H. Daldrup-Link (✉)
Department of Radiology,
University of California, San Francisco,
505 Parnassus Ave,
San Francisco, CA, 94143–0628, USA
e-mail: daldrup@radiology.ucsf.edu
Tel.: +1-415-4762306
Fax: +1-415-4760616

S. C. Chawla
Olive View-UCLA Medical Center,
Department of Radiological Sciences
2D115, 14445 Olive View Drive,
Sylmar, CA, 91342, USA

Abstract Hepatic masses constitute about 5–6% of all intra-abdominal masses in children. The majority of liver tumors in children are malignant; these malignant liver tumors constitute the third most common intra-abdominal malignancy in the pediatric age group after Wilms' tumor and neuroblastoma. Only about one third of the liver tumors are benign. A differential diagnosis of liver tumors in children can be obtained based on the age of the child, clinical information (in particular AFP) and imaging characteristics. The purpose of this review is to report typical clinical and imaging characteristics of benign and malignant primary liver tumors in children.

Keywords Pediatric liver tumors · Hepatoblastoma · Hepatocellular carcinoma · FNH · Adenoma · Mesenchymal hamartoma

Benign tumors

Infantile hepatic hemangioma or hemangioendothelioma

Hepatic hemangiomas and hemangioendotheliomas are the most common vascular hepatic tumors in the first year of life (50% of the benign tumors) [1, 2]. Up to 85% of these tumors present by 6 months of age, the male:female ratio being 1:2. These tumors may grow rapidly in the perinatal period and may involute eventually. Occasionally, almost the entire liver may be involved with hemangioendotheliomas with little sparing of liver parenchyma. The two lesions show distinct histopathological characteristics. Infantile hepatic hemangiomas are benign vascular lesions. Epitheliod hemangioendotheliomas are also primarily benign, endothelium lined vascular masses, but may show a malignant potential [3]. In the proliferative phase, there is characteristic hypercellularity, endothelial proliferation and dilatation of vascular spaces, leading to a characteristic 'cavernous appearance'.

Hemangioendotheliomas are usually associated with mild elevations in AFP levels (around 10,000 units). Thus, this may help in differentiating the mass from a hepatoblastoma which have markedly elevated AFP levels [3]. Endothelial growth factor is positive [4]. Additional vascular malformations are commonly seen in the skin, bone and other organs. Infantile hemangiomas may produce type-3 iodothyronine deiodinase leading to hypothyroidism [5]. Epitheliod hemangioendotheliomas may present with consumptive coagulopathy, which may result in disseminated intravascular coagulation (DIC), also known as Kasabach-Merritt syndrome [2]. Extensive arterio-venous shunting can lead to high output congestive heart failure.

On ultrasound (US), infantile hemangiomas and hemangioendotheliomas are well circumscribed, hypo- or hyperechoic nodules (Fig. 1), which may show flow in vascular structures on Doppler US. In contrast to adult hemangiomas, only a few of these lesions will be hyperechoic. Multiple lesions are common in hemangioendotheliomas. On unenhanced computed tomography (CT), hemangio-

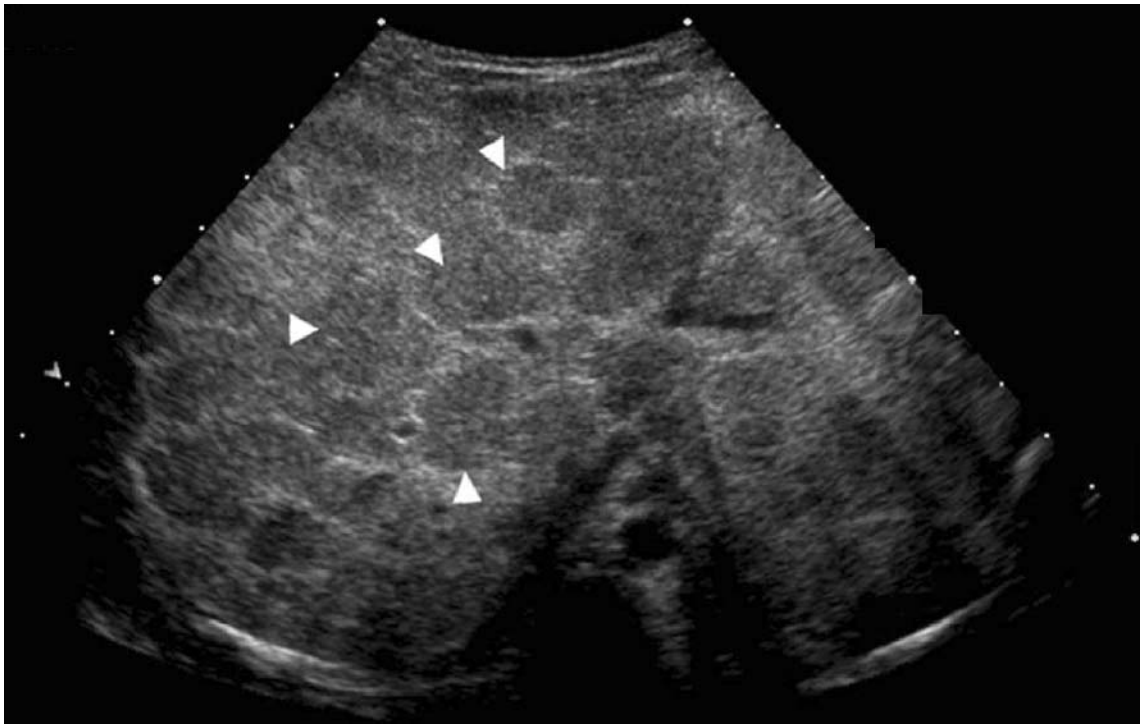

Fig. 1 A 7-month-old girl with hemangioendothelioma of the liver. The patient also had hemangiomas of the skin. An infection and a malignancy, in particular neuroblastoma, were ruled out by laboratory and imaging studies. In this setting, multiple lesions suggest the diagnosis of hemangioendothelioma. US image through the liver demonstrates multiple, well-circumscribed hypoechoic nodules (*arrowheads*)

mas and hemangioendotheliomas have a lower attenuation than the liver parenchyma with occasional hemorrhage (Fig. 2a). Calcifications may be seen in up to 40% of cases. On contrast-enhanced CT there is a characteristic intense, nodular peripheral rim enhancement with central progression (Fig. 2b,c). Central filling defects may occur in larger lesions due to central thrombosis or fibrosis. On delayed enhanced images, infantile hemangiomas and hemangioendotheliomas show a characteristic persistent enhancement, a distinct feature compared with other liver tumors.

On MR images, infantile hemangiomas and hemangioendotheliomas show a very high signal intensity (similar to cerebrospinal fluid as an internal standard) on T2WI (Figs. 2d, 3a,b) and are typically hypointense compared with liver parenchyma on T1-weighted images (T1WI) (Fig. 2e) [6]. Flow voids due to enlarged feeding and draining vessels may be seen leading to and from the lesions (Fig. 2e). Contrast-enhanced MR images show a similar enhancement pattern compared with contrast-enhanced CT images, as described above (Fig. 2f,g).

Mesenchymal hamartoma

This benign developmental liver tumor is the second most common benign hepatic lesion in the perinatal period. It is seen usually in children less than 2 years of age with a male:female ratio of 2:1. The tumor arises from mesenchymal tissue around the portal tract. Grossly, the lesion is not encapsulated and is typically composed of multiple cysts, filled with clear or mucoid fluid. Calcifications are rare. A rarer variant is a predominantly solid lesion with cystic areas producing a Swiss cheese pattern [7, 8].

Imaging findings depend on stromal tissue content of the lesion. On US, the tumor presents as a large multiseptated cystic mass. Rarely, the tumor may appear solid or may contain echogenic material secondary to hemorrhage. CT images show a multilocular low-attenuation cystic mass with enhancing septae and stroma (Fig. 4a,b). Calcification is generally not seen.

Magnetic resonance imaging (MRI) demonstrates a characteristic, very high signal on T2WI (similar to cerebrospinal fluid as an internal standard) in the cystic areas (Fig. 5a). Septae and focal areas of stromal tissue may remain hypointense on T2WI. On T1WI (Fig. 5b) the cystic components of the tumor show a variable signal intensity, homogeneously hypointense, isointense or hyperintense compared with surrounding liver tissue, depending on variable protein content. As with CT, the mass typically shows only a peripheral rim enhancement (Fig. 5c). Predominantly solid mesenchymal hamartomas are hy-

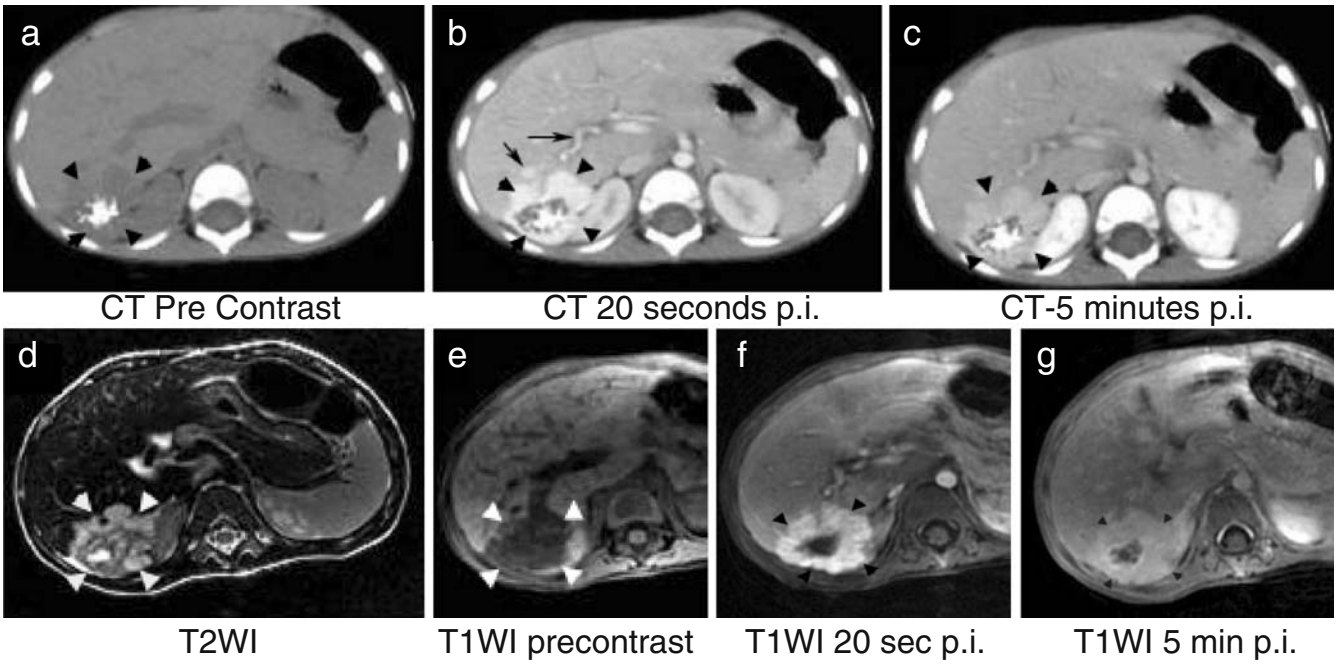

Fig. 2 A 20-month-old girl with hemangioedothelioma. **a** Unenhanced axial CT slice with soft tissue window. The tumor (*arrowheads*) is seen as a well-defined, lobulated, low attenuation mass in the right lobe of the liver. Hyperintensity in the center of the lesion represents dystrophic calcification. **b** Axial CT post contrast in venous phase. A feeding artery (*horizontal arrow*) and a draining vein (*slanting arrow*) are delineated and the lesion enhances centripetally. **c** Enhanced axial CT 5 min after contrast medium administration shows persistent enhancement with hyperdensity of the lesion relative to the surrounding liver parenchyma, a feature characteristic for a hemangioendothelioma. **d** Axial T2WI demonstrate the tumor to have a typical lobulated contour and a very high signal intensity. **e** Axial T1WI demonstrates a well-defined, low intensity mass (*arrowheads*) which enhances upon contrast. Of note, the central calcification is not apparent on MR. **f** Axial T1WI after contrast medium administration shows intense enhancement of the tumor in the early phase. **g** Axial T1WI shows persistent enhancement on delayed imaging

pointense to liver parenchyma on T1WI and slightly hyperintense on T2WI (Fig. 5a–c). The solid variant may not be distinguishable from hepatoblastomas based on imaging characteristics.

Hepatic adenomas

Adenomas are rare in the pediatric population and constitute 6% of all benign pediatric hepatic tumors.

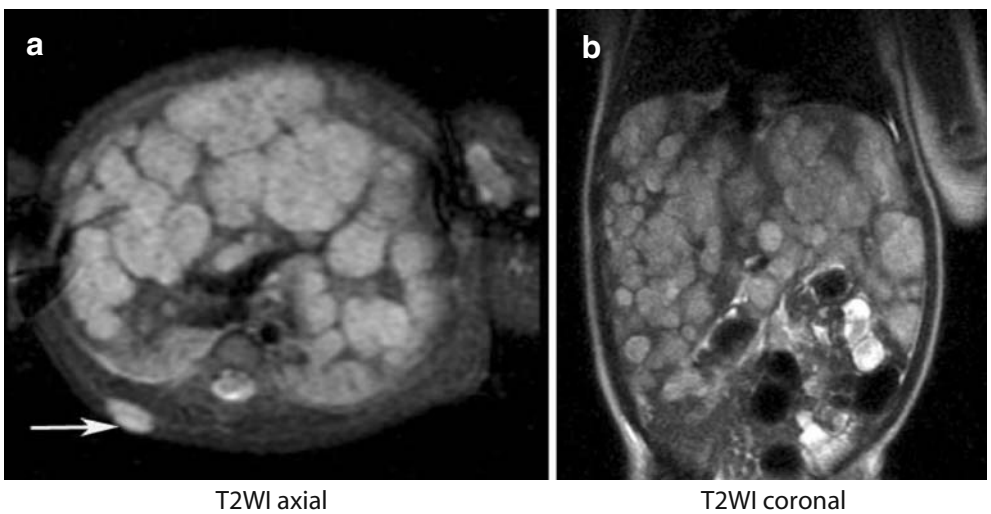

Fig. 3 A 12-month-old baby with multiple hemangioendotheliomas. The entire liver is seen to be involved with limited sparing of the liver parenchyma. **a** Axial T2-weighted images (T2WI). The lesions have a very bright signal. A subcutaneous hemangioma is also noted (*arrow*). **b** Coronal T2WI

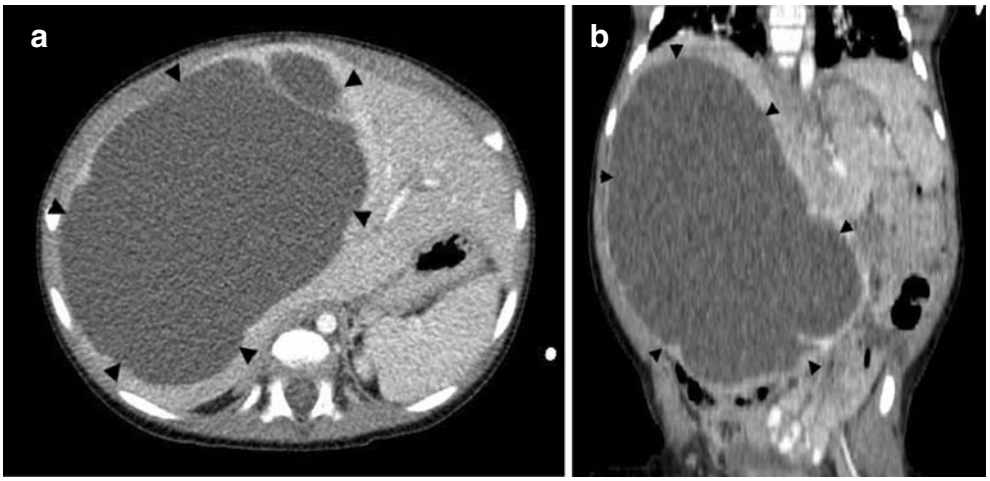

Fig. 4 Huge mesenchymal hamartoma in a 12-month-old girl. The patient presented with abdominal distension. **a** On enhanced CT, a cystic multiseptated mass has replaced most of the liver parenchyma. Only the stromal components enhance on contrast. **b** On coronal reformats the mass was noted to occupy large areas in the abdomen

They are usually seen in teenagers with a female preponderance. They may be seen in patients with glycogen-storage diseases. Hepatic adenomatosis is defined as four or more adenomas seen with oral contraceptive and anabolic steroid use.

Histologically, adenomas present as encapsulated, rounded masses, which consist of hepatocytes, Kupffer cells, rudimentary portal tracts and distorted biliary elements. Of note, the Kupffer cells in adenomas have a decreased or absent phagocytic activity, a distinctive feature compared with FNHs. Adenomas may be asymptomatic or present with abdominal pain or an acute large hemorrhage. Adenomas may show malignant degeneration.

On US, adenomas can be difficult to diagnose since they are usually nearly isoechoic to liver parenchyma. CT demonstrates an isodense or slightly hypodense mass with a well-defined border due to the presence of a capsule. Hemorrhage may lead to a heterogeneous appearance. After intravenous contrast medium administration, adenomas typically show an early arterial enhancement followed by a rapid wash-out.

On unenhanced MR images, adenomas typically have a very similar signal intensity compared with surrounding liver parenchyma. They may be isointense or slightly hyperintense on T2WI as well as isointense or slightly hypointense on T1WI [6]. Hemorrhage within the tumor may cause more complex signal characteristics. Gadolinium-based contrast agents provide similar enhancement patterns as described for CT. Unlike FNH, central heterogeneities in adenomas (e.g., fibrosis) do not show an enhancement on delayed post contrast images. Adenomas show characteristically no or only minimal uptake of iron oxide contrast agents (Feridex/Endorem) due to inactive Kupffer cells within the lesions [9–13]. Adenomas appear hypointense compared with liver parenchyma on delayed MR images after injection of the hepatobiliary contrast agent Gd-BOPTA (gadobenate dimeglumine Multihance) [14].

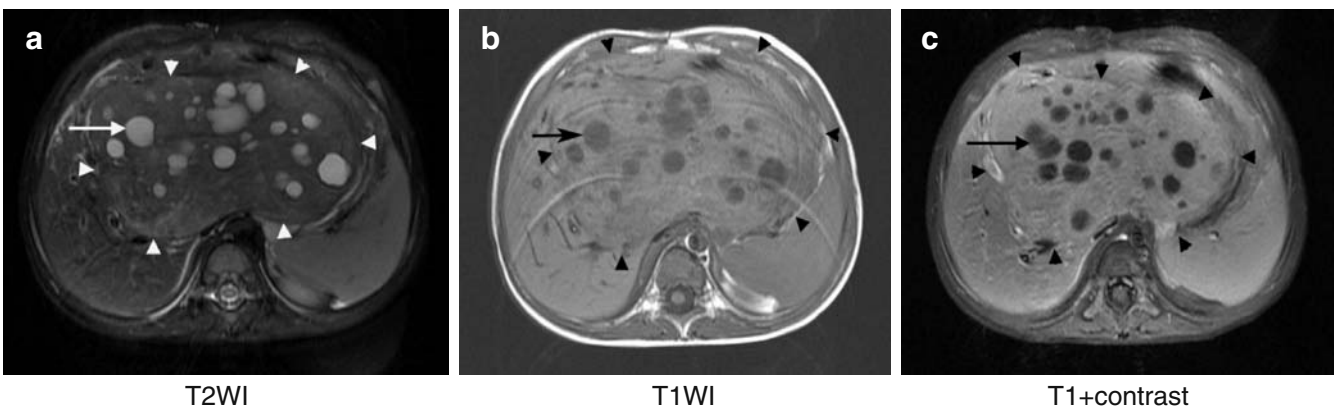

Fig. 5 A 15-month-old child with mesenchymal hamartoma (solid variant). The tumor is seen as a predominantly solid mass with cystic areas. **a** On T2WI the cystic areas have very high signal intensity. The solid componenet is slightly hyperintense to the liver in this phase. **b** On T1WI the tumor is isointense to hypointense with hypointense cystic areas. **c** Following administration of contrast medium, the tumor enhances similar to liver parenchyma but the cysts fail to enhance

Focal nodular hyperplasia (FNH)

FNHs constitute 5% of benign liver tumors in children. They present almost exclusively in girls. Two age peaks have been described, around 6 years and 18 years. FNHs may develop based on a congenital AVM or due to iatrogenic hepatic vascular abnormalities, e.g., after chemotherapy or after Kasai procedures for biliary atresia. Multiple FNHs have been reported in type I glycogen storage disorder.

The causal arterio-venous malformation forms a central nidus, which develops into a central, vascularized scar. Histology shows hyperplastic hepatocytes, small bile ducts, active Kupffer cells and lymphocytic infiltrates. FNHs are often asymptomatic and detected as an incidental finding.

On US, FNHs are non-encapsulated, solitary masses (rarely multiple) with variable echogenecity, very similar to surrounding liver tissue. The central scar is seen in about one-third of the cases. On CT, FNHs are typically nearly isodense to surrounding liver parenchyma. After intravenous contrast medium administration, FNHs show an early, rapid and short enhancement in the arterial phase (Fig. 6a, b) with a rapid washout (Fig. 6c). The central scar appears hypodense compared with enhancing liver parenchyma on early enhanced images and hyperdense due to retained contrast in the central vascular malformation on delayed CT imaging (characteristic for FNH). On MR images, FNHs have a very similar signal intensity compared with surrounding liver parenchyma on all pulse sequences, being isointense or slightly hyperintense on T2WI as well as isointense or slightly hypointense on T1WI. Central scars are hypointense with respect to the main lesion on T1WI and hyperintense on T2WI. The contrast enhancement is similar to that described for CT above. Characteristic is an uptake of iron oxide contrast agents (Feridex/Endorem) [9–11]. FNHs appear hyperintense or isointense compared with liver parenchyma after injection of Gd-BOPTA [15, 16].

Malignant tumors

Hepatoblastoma

Hepatoblastomas are the most common primary liver tumors in young children with a peak presentation at 1–2 years of age and a male:female ratio of 2:1 [2]. Less frequently, hepatoblastomas may also occur in older children, up to 15 years of age. Predisposing conditions include Beckwith-Wiedemann syndrome, hemihypertrophy, familial polyposis coli, Gardner's syndrome, fetal alcohol syndrome and Wilms' tumor. It has also been reported to be present more commonly in premature infants and low birth weight infants [17].

Histologically, the tumor presents as a large, usually solitary, solid mass. It may contain fibrous bands, leading to a 'spoked-wheel appearance'. Histologically, the tumor can either be epithelial or mixed type. The tumor has a tendency to invade hepatic and portal veins. Serum AFP is typically raised in 90% of patients with hepatoblastoma and not elevated in about 10%

On US, hepatoblastomas are solid masses with similar signal intensity compared with surrounding liver parenchyma. The typical spoked-wheel appearance as a result of fibrous septae may be rarely appreciated. Calcification is seen in 55% of cases and may cause acoustic shadowing. Additional intralesional necroses or tumor thrombi in the portal vein or hepatic veins may be seen. Unenhanced CT typically shows a relatively well-defined, heterogeneous mass, slightly hypodense compared with liver tissue, with or without calcifications. On contrast-enhanced CT, the tumor reveals a heterogeneous enhancement (Fig. 7a,b), which may be hyperdense compared with liver parenchyma in the early arterial postcontrast phase and usually appears iso- or hypodense on delayed images. Invasion of the portal vein and its subsequent thrombosis must be evaluated in all suspected cases of hepatoblastoma. The tumor thrombus can even spread along IVC and encroach

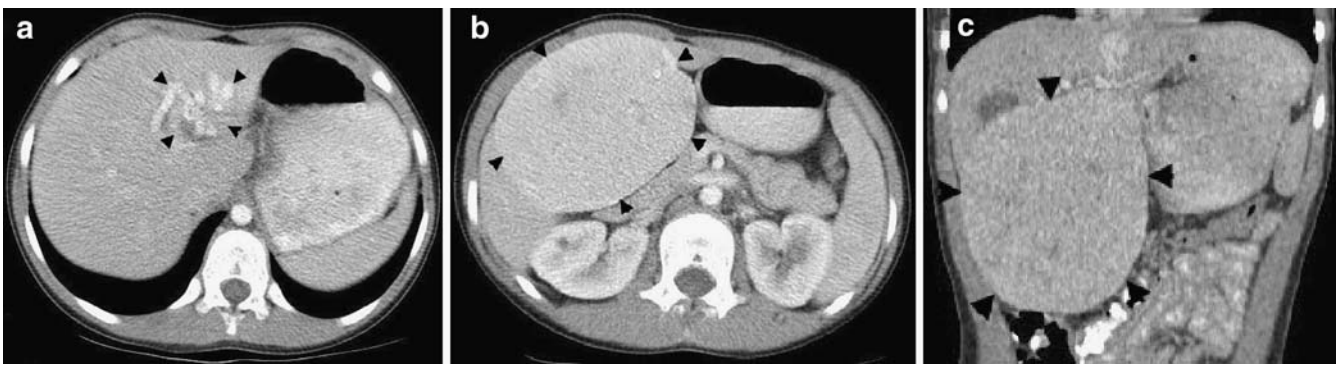

Fig. 6 A 9-year-old girl with large, pedunculated FNH. **a** Axial CT of the abdomen (soft tissue window) in the early postcontrast phase demonstrates the vascular malformation (*arrowheads*) forming the nidus of the tumor. **b** The tumor enhances intensely and uniformly in the early arterial phase, followed by rapid wash-out. **c** Coronal CT image depicts the mass to be huge and pedunculated

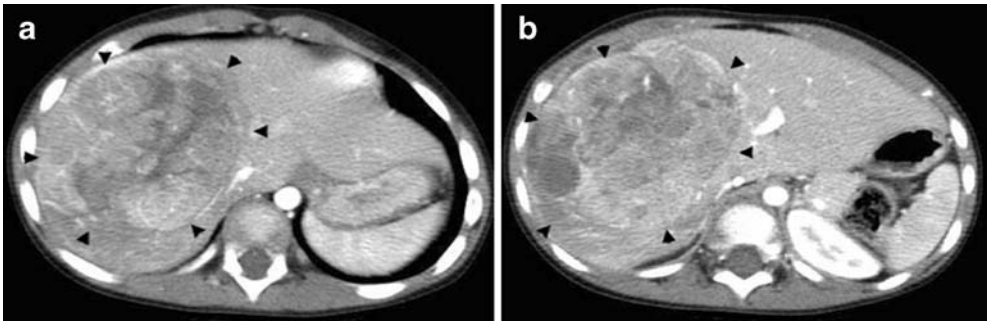

Fig. 7 **a**, **b** A 3-year-old boy with hepatoblastoma. Axial enhanced CT images of the abdomen demonstrate an ill-defined heterogeneous mass (*arrowheads*) with areas of necrosis appearing hypodense to the liver parenchyma

in the lumen of right atrium. Metastasis may be seen in lymph nodes and lung parenchyma, rarely in the bones and brain. On MR, hepatoblastomas are iso- or slightly hyperintense on T2WI (Fig. 8a) and iso- or hypointense compared with liver parenchyma on T1WI (Fig. 8b). Central necrosis may show a high T2-signal. The contrast enhancement of hepatoblastomas is similar compared with CT and quite non-specific. The enhancement of hepatoblastomas with iron oxides or hepatobiliary contrast agents has not yet been described.

Hepatocellular carcinoma (HCC)

HCC typically affects children over 10 years of age with no specific sex predilection. Conditions predisposing to cirrhosis such as biliary atresia, infantile cholestasis, hemochromatosis, hereditary tyrosinemia, glycogen storage disorders and hepatitis B infection are associated with HCC. AFP is elevated in about 50% of the cases and beta HCG levels may be raised.

Histologically, two forms are seen, classic and fibrolamellar HCCs. In the latter, tumor cells are circumscribed by bundles of acellular collagen. This form is seen more frequently in adolescents than in the adult populations and has a better prognosis.

On US, HCCs show a similar echogenecity compared with liver parenchyma, they are usually minimally hyperechoic (Fig. 9a,b). Calcifications are seen in about 40% of the cases. On CT, HCCs present with highly variable and non-characteristic features: the tumors may be homogeneous or heterogeneous, solitary or multifocal, well- or ill-defined. HCCs are typically isodense or slightly hypodense compared with liver parenchyma on unenhanced CT images and show an early arterial contrast enhancement and a rapid wash-out on enhanced CT (Fig. 9c). HCCs are often inconspicuous on delayed scans. Invasion of portal veins, hepatic veins, hepatic arteries and inferior vena cava may be seen. The diagnosis of an underlying cirrhosis may help in the differential diagnosis, but is rare in children. Diffuse involvement of the liver leads to a diffusely hypodense liver on CT. HCCs metastasize to lung, bone, skin and brain. On MR, HCCs likewise show highly variable and non-characteristic imaging features. As primary liver lesions, HCCs show similar signal intensities compared with liver parenchyma, being slightly hyperintense on T2WI (Fig. 10a) and iso- or slightly hypointense on T1WI (Fig. 10b) [6]. A heterogeneous enhancement is noted with gadolinium administration, similar to CT (Fig. 10c). The uptake of cell specific, iron oxide-based or hepatobiliary contrast agents is dependent on the differentiation of the underlying tumor cells [16, 18, 19]. Most HCCs show no enhancement with iron oxides, Mn-DPDP, and Gd-BOPTA on delayed enhanced MR. However, well differentiated HCCs may show an enhancement with these agents. Hence, the imaging features of HCC in the pediatric population are not markedly different from those seen in adults.

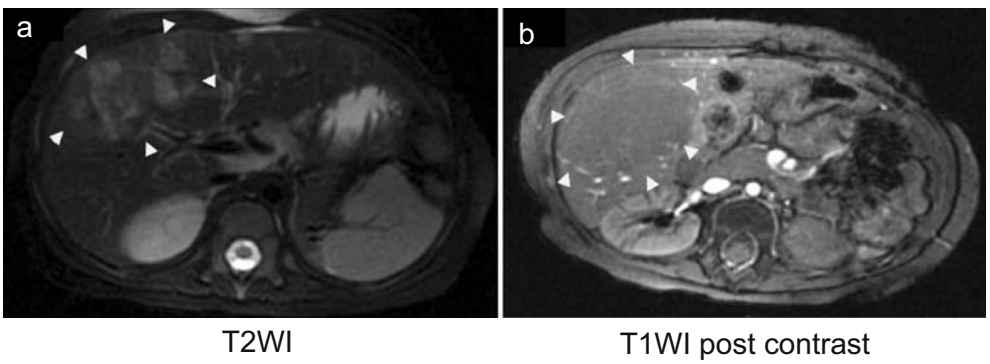

Fig. 8 A 2-year-old boy with hepatoblastoma. **a** Axial T2WI MR image of the abdomen depicts a mass (*arrowheads*) in the right lobe of liver which is slightly hyperintense to the liver parenchyma. **b** Axial T1W MR image of abdomen. The mass is hypointense to the normal liver parenchyma

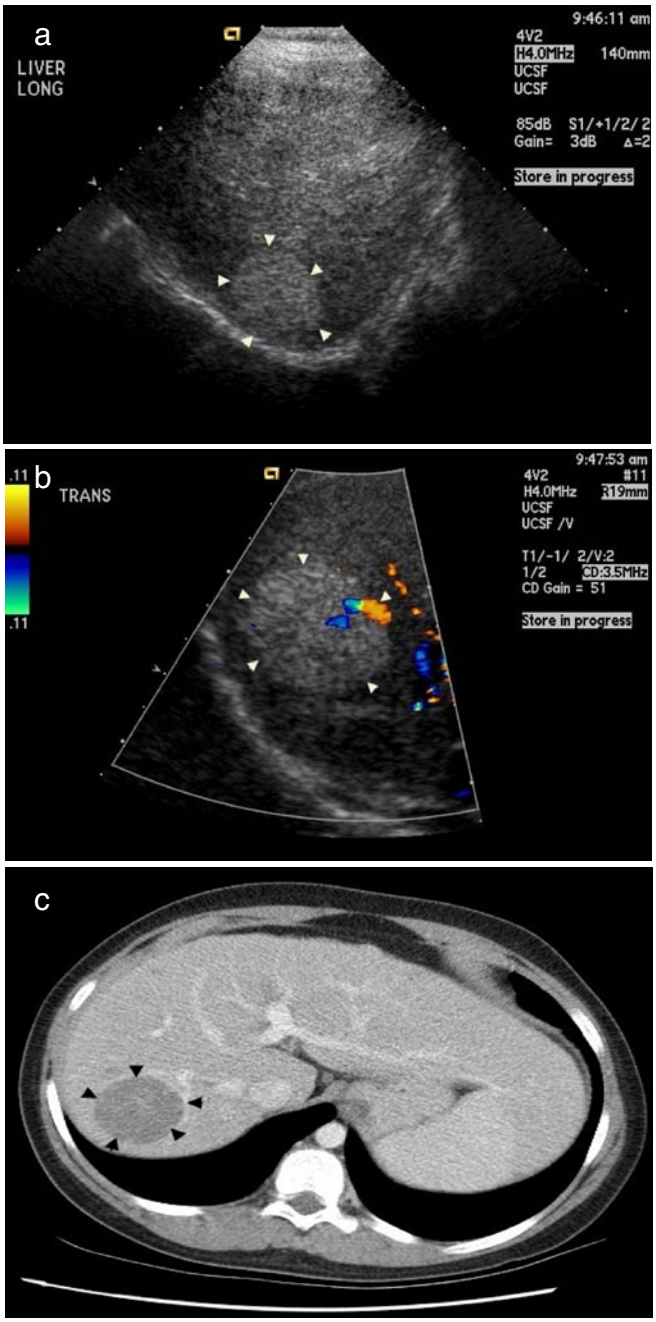

Fig. 9 A 9-year-old boy with previously diagnosed neonatal hepatitis B infection with hepatocellular carcinoma. **a**, **b**. US abdomen. The tumor is seen as a well-defined, hyperechoic mass (*arrowheads*) **c** Contrast-enhanced axial CT. The mass is hypodense in comparison with the liver parenchyma and shows early enhancement followed by rapid wash-out upon contrast administration. Of note, the liver is not cirrhotic as opposed to that seen in adults

Undifferentiated (embryonal) sarcoma

Undifferentiated (embryonal) sarcoma is a rare primary malignant tumor of the liver that typically presents in later childhood, in children with a mean age of 6–10 years. Undifferentiated (embryonal) sarcomas are very aggressive tumors with a high potential for local recurrence and distant metastasis.

There is a documented conversion of a mesenchymal hamartoma to an undifferentiated embryonal sarcoma. Thus, it is currently debated, if the undifferentiated embryonal sarcoma is the malignant counterpart of a mesenchymal hamartoma [20–22]. The AFP is usually in the normal range in these patients, which may help in the differential diagnosis from hepatoblastomas [2, 23]. Undifferentiated (embryonal) sarcomas are predominantly solid lesions with central necrosis or hemorrhage.

A discrepancy between the US and CT appearance is the hallmark of diagnosis of undifferentiated embryonal sarcomas. US typically shows an inhomogeneous, multiseptated solid tumor (Fig. 11a,b). CT demonstrates a large markedly hypodense, apparently predominantly cystic mass due to the myxoid component of the tumor [2]. This mass shows no or only a peripheral rim enhancement on early enhanced CT (Fig. 11c,d), and a slow, partial enhancement of some tumor areas on delayed images. On MRI, the tumor is heterogeneous and has a very high signal on T2WI and a low signal on T1WI. The tumor shows a peripheral enhancement of a surrounding pseudocapsule of compressed liver tissue and septae on early enhanced MR, and may show enhancement of tumor nodules on delayed imaging. Metastases may be seen in lung and bone, brain and skin.

CT and MRI in pediatric liver tumors: Technical aspects

Pediatric patients present unique technical challenges for both CT and MRI. Apart from the radiation involved in CT, sedation and general anesthesia are important factors in planning and performing these studies [24, 25].

CT

Technical differences in CT imaging for liver tumors in children as compared with adults focus on reduction of the radiation burden, primarily by eliminating unenhanced CT and by using multiphase contrast studies only in few selected cases [26–29]. The CT parameters used in our institution include: slice thickness ranges from 2.5 to 5 mm, pitch 1.0–1.5, 80–120 kVp and 120–140 mAs [30–32]. Contrast agent details are summarized in Table 1 [33, 34].

MRI

A detailed discussion about sedation planning is beyond the scope of this article. In general, however, there is a window of 30–60 min for MRI with sedated child and MR

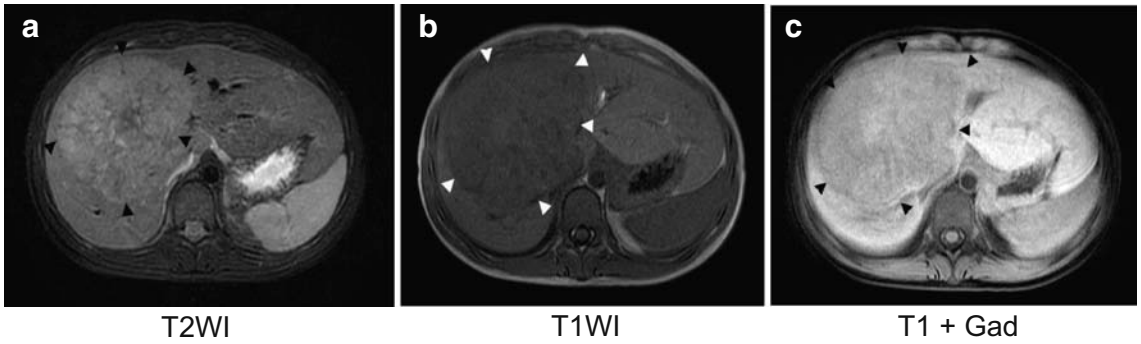

Fig. 10 A 15-year-old girl with a hepatocellular carcinoma (fibrolamellar variant). **a** Axial T2WI. The tumor (*arrowheads*) is seen to be hyperintense to the liver parenchyma. **b** Axial T1WI. The tumor (*arrowheads*) is hyperintense to the liver. **c** Contrast-enhanced T1WI. The tumor (*arrowheads*) enhances with intravenous contrast medium, but still remains hypointense to the liver parenchyma

sequences should be tailored to get the maximum possible information [25]. For neonates and infants knee or head coils are used, whereas for older children a body-phased array coil is utilized. Dynamic contrast-enhanced scans using gadolinium chelates are an integral part of the study. Sequences differ with each individual case and with the age of the child. In general, the following sequences are performed in most cases: three-plane localizer, T2 SSFSE

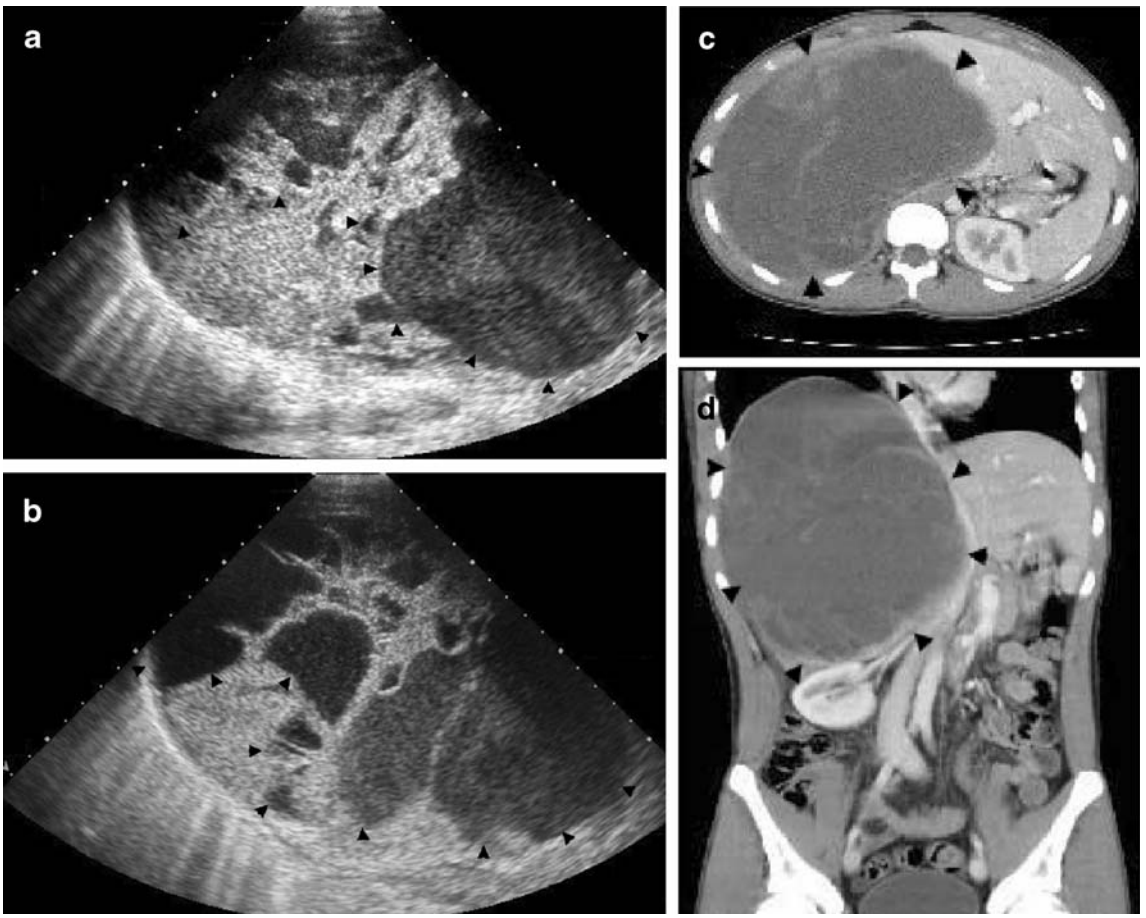

Fig. 11 A 17-year-old boy with undifferentiated embryonal sarcoma who presented with breathing difficulty and right upper quadrant abdominal pain. **a**, **b** US image through the liver demonstrates a heterogeneous, predominantly solid appearing multiseptated mass (*arrowheads*) in the right lobe of liver. **c** Axial contrast-enhanced CT images through the liver demonstrate a large well defined, apparently cystic mass (*arrowheads*) in the right lobe of the liver with minimal enhancement. This discrepancy between the CT and US appearance is the hallmark for diagnosis for this tumor. **d** Coronal contrast-enhanced CT of the abdomen

Table 1 Contrast agents used in CT and MRI: technical aspects [34, 35, 37]

	CT	MRI
Type	Low osmolality, non ionic most commonly used	Gadolinium chelates
Volume	2-3 ml/kg	0.1–0.2 mmol/kg
Rate	Depending on the bore of IV access varies from 0.5 to 2 ml/s	0.5–2 ml/s (as for CT)
Scan delay	15–20 s after the completion of injection or using Smart Prep to coincide with peak hepatic enhancement	Immediately after injection

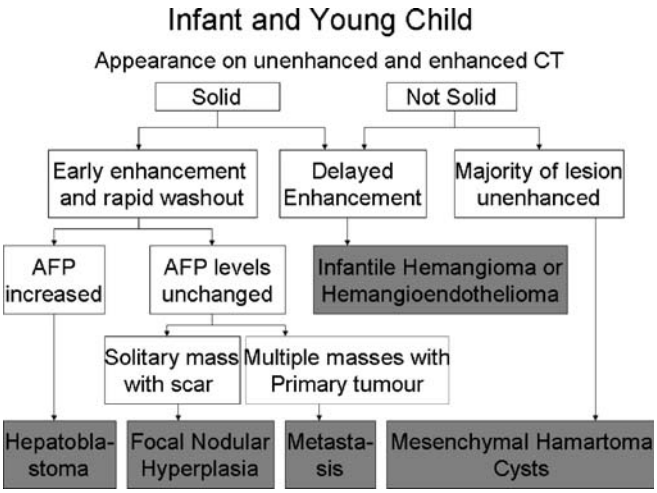

axial and coronal images, T1 FSE axial and coronal images (if breath-hold is possible) and dynamic multiphase (precontrast, arterial, portal and parenchymal phase) spoiled gradient echo axial images (LAVA, THRIVE, FAME, VIBE). Additional imaging, including three-dimensional TOF angiography, venography, dual-phase GRE imaging and MRCP, may be performed to answer specific questions [35, 36]. The use of intracellular MRI contrast agents has not yet been approved in pediatric patients (Table 1) [24, 37].

Review of MR spectroscopy (MRS) in liver tumors

MRS has been used for more than two decades to interrogate metabolite distributions in living cells and tissues and has been used to investigate cardiac and skeletal muscle energetics, neurobiology, and cancer [38]. Proton MRS is widely used both as a clinical and research tool, in the evaluation of benign and malignant lesions of the brain. However, MRS is not routinely used for diagnosis of liver tumors. In-vivo proton MRS has potential in the detection of early metabolite change in malignant liver tumors after transcatheter arterial chemoembolization (TACE) but a limitation exists in clear differentiation between normal liver and benign and malignant tumor [39]. The quantification of choline-containing compounds (Cho) in hepatic tumors by ^{1}H MRS is of great interest because such compounds have been linked to malignancy and the method of quantification of choline compounds in human hepatic tumors by proton MRS at 3 T may be a promising technique for evaluating response to treatment in liver cancer [40]. Liver tumors have increased phosphomonoester (PME) and effective treatment is often associated with its diminished level [41]. The results from in-vivo clinical work on hepatic tumors from a number of research groups show clearly that, although in-vivo ^{31}P MRS can be used to distinguish between normal and neoplastic tissue, it cannot

Table 2 Follow-up imaging for liver tumors: summary based on the ACR appropriateness criteria scale (range 1–9, where 1 = least appropriate, 9 = most appropriate) [43]

	No further imaging, consider follow up	US	MR	CT	Biopsy	Comment
Typical benign on imaging, no history of malignancy	8	5	4	4	2	Mesenchymal hamarthoma needs surgery
Typical benign on imaging, known history of malignancy	8	5	5	5	2	
Typical malignant on imaging,	7	4	6	6	7	Follow-up and further imaging
>1 cm indeterminate on imaging, no history of malignancy	-	5	8	8	5	
>1 cm indeterminate solid mass on imaging, history of malignancy	-	5	7	7	8	
<1 cm indeterminate solid mass on imaging	8	7	5	5	2	

be used to discriminate between different tumor types, or for separating benign from malignant neoplasms. A key function for in-vivo MRS will, however be in the monitoring of tumor response to therapy [42].

Conclusion

Primary liver tumors are rare in the pediatric population. US is the initial investigation modality of choice. Both CT and MRI may be used for evaluating the extent of the tumor for further evaluation, to acquire additional information for differential diagnoses and to diagnose metastases to lung, lymph nodes or bone. CT requires less or no anesthesia due to faster scan times. MRI has the advantage over CT of reducing radiation exposure in children and to provide more specific diagnoses, especially with the use of new, cell-specific contrast agents. The final diagnosis and characterization of liver masses should be made in a stepwise approach, considering characteristic clinical data (age of the patient), AFP levels and imaging features. The imaging modality and time interval for follow-up studies largely depends on the clinical situation. US is the modality of choice for the follow-up of hemangioendotheliomas. These may involute with calcifications, which can create technical problems in follow-up with sonography. In such instances and in case of iso-echogenic FNH or adenomas,

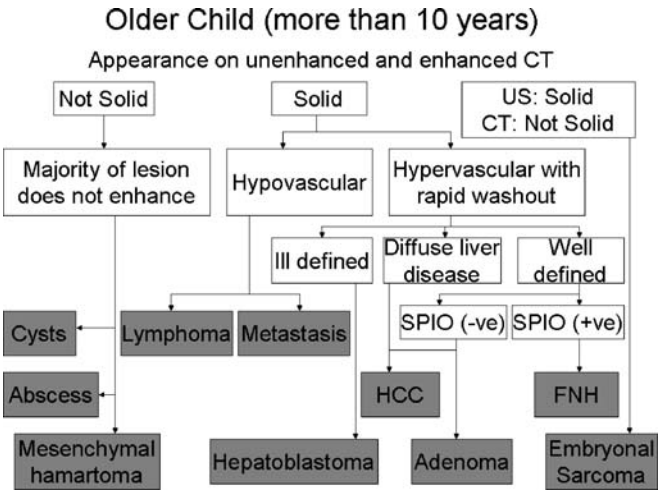

MR or CT may be added. At our institution, follow-up studies of malignant liver lesions under chemotherapy or before and after surgery are performed with cross-sectional imaging modalities, although we sometimes add adjunctive, interim or short term follow-up US studies. For adults, the American College of Radiology (ACR) created guidelines for the appropriate follow-up of focal liver lesions, which may be also considered to some extent for pediatric patients (Table 2) [43].

References

1. Kuhn JP, Slovis TL, Haller JO, Caffey J (eds) (2004) Caffey's pediatric diagnostic imaging, 10th edn. Mosby, Philadelphia
2. Helmberger TK, Ros PR, Mergo PJ et al (1999) Pediatric liver neoplasms: a radiologic-pathologic correlation. Eur Radiol 9:1339–1347
3. Emre S, McKenna GJ (2004) Liver tumors in children. Pediatr Transplant 8:632–638
4. Szymik-Kantorowicz S, Partyka L, Dembinska-Kiec A et al (2003) Vascular endothelial growth factor in monitoring therapy of hepatic haemangioendothelioma. Med Pediatr Oncol 40:196–197
5. Ayling RM, Davenport M, Hadzic N et al (2001) Hepatic hemangioendothelioma associated with production of humoral thyrotropin-like factor. J Pediatr 138:932–935
6. Schneider G, Grazioli L, Saini S (eds) (2003) MRI of the liver: imaging techniques, contrast enhancement, differential diagnosis. Springer, Milan, New York, p 214
7. Stringer MD, Alizai NK (2005) Mesenchymal hamartoma of the liver: a systematic review. J Pediatr Surg 40:1681–1690
8. Chang HJ, Jin SY, Park C et al (2006) Mesenchymal hamartomas of the liver: comparison of clinicopathologic features between cystic and solid forms. J Korean Med Sci 21:63–68
9. Bartolotta TV, Midiri M, Galia M et al (2001) Benign hepatic tumors: MRI features before and after administration of superparamagnetic contrast media. Radiol Med (Torino) 101:219–229
10. Beets-Tan RG, Van Engelshoven JM, Greve JW (1998) Hepatic adenoma and focal nodular hyperplasia: MR findings with superparamagnetic iron oxide-enhanced MRI. Clin Imaging 22:211–215
11. Kim MJ, Kim JH, Lim JS et al (2004) Detection and characterization of focal hepatic lesions: mangafodipir vs. superparamagnetic iron oxide-enhanced magnetic resonance imaging. J Magn Reson Imaging 20:612–621
12. Mergo PJ, Engelken JD, Helmberger T et al (1998) MRI in focal liver disease: a comparison of small and ultra-small superparamagnetic iron oxide as hepatic contrast agents. J Magn Reson Imaging 8:1073–1078
13. Urhahn R, Adam G, Busch N et al (1996) Superparamagnetic iron oxide particles: what value has the T1 effect in the MR diagnosis of focal liver lesions? Rofo 165:364–370

14. Pena CS, Saini S, Baron RL et al (2001) Detection of malignant primary hepatic neoplasms with gadobenate dimeglumine (Gd-BOPTA) enhanced T1-weighted hepatocyte phase MR imaging: results of off-site blinded review in a phase-II multicenter trial. Korean J Radiol 2:210–215
15. Frohlich JM (2004) MRI of focal nodular hyperplasia (FNH) with gadobenate dimeglumine (Gd-BOPTA) and SPIO (ferumoxides): an intra-individual comparison. J Magn Reson Imaging 19:375–376 author reply 376
16. Grazioli L, Morana G, Kirchin MA et al (2003) MRI of focal nodular hyperplasia (FNH) with gadobenate dimeglumine (Gd-BOPTA) and SPIO (ferumoxides): an intra-individual comparison. J Magn Reson Imaging 17:593–602
17. Maruyama K, Ikeda H, Koizumi T et al (2000) Case-control study of perinatal factors and hepatoblastoma in children with an extremely low birthweight. Pediatr Int 42:492–498
18. Tanimoto A, Kuwatsuru R, Kadoya M et al (1999) Evaluation of gadobenate dimeglumine in hepatocellular carcinoma: results from phase II and phase III clinical trials in Japan. J Magn Reson Imaging 10:450–460
19. Hamm B, Kirchin M, Pirovano G et al (1999) Clinical utility and safety of MultiHance in magnetic resonance imaging of liver cancer: results of multicenter studies in Europe and the USA. J Comput Assist Tomogr 23(Suppl 1): S53–S60
20. Lauwers GY, Grant LD, Donnelly WH et al (1997) Hepatic undifferentiated (embryonal) sarcoma arising in a mesenchymal hamartoma. Am J Surg Pathol 21:1248–1254
21. O'Sullivan MJ, Swanson PE, Knoll J et al (2001) Undifferentiated embryonal sarcoma with unusual features arising within mesenchymal hamartoma of the liver: report of a case and review of the literature. Pediatr Dev Pathol 4:482–489
22. Ramanujam TM, Ramesh JC, Goh DW et al (1999) Malignant transformation of mesenchymal hamartoma of the liver: case report and review of the literature. J Pediatr Surg 34:1684–1686
23. Craig JR (1994) Mesenchymal tumors of the liver. Diagnostic problems for the surgical pathologist. Pathology (Phila) 3:141–160
24. Boechat MI, Kangarloo H (1989) MR imaging of the abdomen in children. AJR Am J Roentgenol 152:1245–1250
25. White KS (1996) Reduced need for sedation in patients undergoing helical CT of the chest and abdomen. Pediatr Radiol 26:5
26. Paterson A, Frush DP, Donnelly LF (2001) Helical CT of the body: are settings adjusted for pediatric patients? AJR Am J Roentgenol 176:297–301
27. Frush DP, Slack CC, Hollingsworth CL et al (2002) Computer-simulated radiation dose reduction for abdominal multidetector CT of pediatric patients. AJR Am J Roentgenol 179:1107–1113
28. Slovis TL (2003) Children, computed tomography radiation dose, and the As Low As Reasonably Achievable (ALARA) concept. Pediatrics 112:971–972
29. da Costa e Silva EJ, da Silva GA (2007) Eliminating unenhanced CT when evaluating abdominal neoplasms in children. AJR Am J Roentgenol 189:1211–1214
30. Frush DP, Donnelly LF (1998) Helical CT in children: technical considerations and body applications. Radiology 209:37–48
31. Vade A, Demos TC, Olson MC et al (1996) Evaluation of image quality using 1:1 pitch and 1.5:1 pitch helical CT in children: a comparative study. Pediatr Radiol 26:891
32. Vade A, Olson MC, Vittore CP et al (1999) Hepatic enhancement analysis in children using Smart Prep monitoring for 2:1 pitch helical scanning. Pediatr Radiol 29:689–693
33. Roche KJ, Genieser NB, Ambrosino MM (1996) Pediatric hepatic CT: An injection protocol. Pediatr Radiol 26:502–507
34. Ruess L, Bulas DI, Kushner DC et al (1998) Peak enhancement of the liver in children using power injection and helical CT. AJR Am J Roentgenol 170:677–681
35. Haliloglu M, Hoffer FA, Gronemeyer SA et al (2000) Three dimensional gadolinium-enhanced MR angiography evaluation of hepatic vasculature in children with hepatoblastoma. J Magn Reson Imaging 11
36. Teo EHJ, Strouse PJ, Prince MR (1999) Applications of magnetic resonance imaging and magnetic resonance angiography to evaluatge the hepatic vasculature in the pediatric patient. Pediatr Radiol 29:238–243
37. Rawsin JV, Seigel MJ (1996) Techniques and strategies in pediatric body MR imaging. Magn Reson Imaging Clin North Am 4:589–598
38. Gillies RJ, Morse DL (2005) In vivo magnetic resonance spectroscopy in cancer. Annu Rev Biomed Eng 7:287–326
39. Kuo YT, Li CW, Chen CY, Jao J, Wu DK, Liu GC (2004) In vivo proton magnetic resonance spectroscopy of large focal hepatic lesions and metabolite change of hepatocellular carcinoma before and after transcatheter arterial chemoembolization using 3.0-T MR scanner. J Magn Reson Imaging 19:598–604
40. Li CW, Kuo YC, Chen CY et al (2005) Quantification of choline compounds in human hepatic tumors by proton MR spectroscopy at 3 T. Magn Reson Med 53:770–776
41. Weiner MW, Hetherington H, Hubesch B et al (1989) Clinical magnetic resonance spectroscopy of brain, heart, liver, kidney, and cancer. A quantitative approach. NMR Biomed 2:290–297
42. Bell JD, Bhakoo KK (1998) Metabolic changes underlying 31P MR spectral alterations in human hepatic tumours. NMR Biomed 11:354–359
43. Foley WD, Bree RL, Gay SB et al (2006) ACR Appropriateness Criteria for liver lesion characterization. American College of Radiology, Reston. Available via http://acsearch.acr.org/VariantList.aspx?topicid=30663. Accessed 31st March 2008